SPANDIDOS PUBLICATIONS

EXPERIMENTAL AND THERAPEUTIC MEDICINE 12: 3979-3987, 2016

Anticancer effects of valproic acid on oral squamous cell carcinoma via SUMOylation *in vivo* and *in vitro*

ZHIJIAN SANG*, YANG SUN*, HONG RUAN, YONG CHENG, XIAOJUN DING and YOUCHENG YU

Department of Stomatology, Zhongshan Hospital, Fudan University, Shanghai 200032, P.R. China

Received August 3, 2015; Accepted September 15, 2016

DOI: 10.3892/etm.2016.3907

Abstract. Aberrant histone deacetylase (HDAC) has a key role in the neoplastic process associated with the epigenetic patterns of tumor-related genes. The present study was performed to investigate the effects and determine the mechanism of action of the HDAC inhibitor, valproic acid (VPA), on the CAL27 cell line derived from oral squamous cell carcinoma (OSCC). The effects of VPA on the viability of CAL27 cells were investigated using MTT assays. Alterations in the cell cycle and apoptosis were also examined using propidium iodide (PI) and Annexin V-PI assays, and were subequently analyzed by flow cytometry. Small ubiquitin-related modifier (SUMO)-related genes were evaluated by reverse transcription-quantitative polymerase chain reaction analysis. In addition, the effects of VPA were assessed using a xenograft model *in vivo*. The present results demonstrated significant dose-dependent inhibition of cell viability following VPA treatment. Treatment with VPA increased the distribution of CAL27 cells in the G_1 phase and reduced cells in the S phase, and significantly increased the expression levels of SUMO1 and SUMO2 ($P<0.01$). Using a xenograft model, the mean tumor volume in VPA-treated animals was demonstrated to be significantly reduced, and the rate of apoptosis was significantly increased, as compared with the control animals. These results suggested that VPA may regulate SUMOylation, producing an anticancer effect *in vivo*. Further investigation into the role of VPA in tumorigenesis may identify novel therapeutic targets for OSCC.

Correspondence to: Dr Xiaojun Ding or Professor Youcheng Yu, Department of Stomatology, Zhongshan Hospital, Fudan University, 180 Fenglin Road, Shanghai 200032, P.R. China
E-mail: dingxiaojun051214@163.com
E-mail: yu.youcheng@zs-hospital.sh.cn

*Contributed equally

Key words: histone deacetylase, valproic acid, CAL27 cells, oral squamous cell carcinoma, small ubiquitin-related modifier

Introduction

Oral squamous cell carcinoma (OSCC) is the most frequent malignant tumor of oral cancer, accounting for at least 90% of all oral malignancies (1). OSCC is a complex disease associated with numerous changes in genetic and epigenetic interactions; however, the mechanisms remain poorly understood (2). Alterations in the histone acetylation/deacetylation balance, have been suggested to underpin the altered gene expression patterns detected in various pathological conditions, including cancer (3) and cardiac hypertrophy (4,5). Histone deacetylases (HDACs) are enzymes that remove acetyl moieties from ε-N-acetylated lysine residues in histones, resulting in chromatin condensation and epigenetic repression of gene transcription. HDACs also catalyse deacetylation of various non-histone proteins, such as the tumor suppressor p53, resulting in the inhibition of its proapoptotic transcriptional activity (6,7). In line with their profound antiapoptotic activity, HDACs are upregulated in various types of cancer and thus are efficiently inhibited by chelating agents. Notably, these HDAC inhibitors (HDACi) have been reported to be successful anticancer agents. Due to their antitumor potential, HDACi have a long history of use in antitumor therapy (8). Previous studies have reported additive effects when HDACi were used *in vitro* to treat prostate cancer cells (9,10). Valproic acid (VPA) is a HDACi with a safety profile that permits its long-term use in patients (11). However few studies have assessed its use in oral cancer. Therefore, knowledge of the effects of VPA on OSCC and its underlying mechanisms may improve understanding of OSCC processes, and provide future therapeutic targets for OSCC patients.

Post-translational modification of proteins can be modulated through acetylation, controlled by HDACs and augmented by small ubiquitin-related modifier (SUMO)-mediated gene regulation (12). Post-translational modification of proteins via conjugation to SUMO-SUMOylation, has been shown to influence protein functions associated with numerous cellular processes, including transcription, signal transduction, subcellular localization and gene expression (13).

SUMOylation is a reversible modification of a dynamic process and SUMO-specific proteases (SENPs) are able to remove SUMO from modified proteins (14). Few studies have examined SUMO modification in oral cancer. Katayama *et al* (15) reported that expression levels of SUMO1 were significantly increased in OSCC tissues and cell lines

compared with normal oral mucosa, and SUMO1 expression was also demonstrated to be correlated with a poor patient prognosis. Ding *et al* (16) reported that SENP5 was increased and associated with tumor differentiation in 48 cases of OSCC, and Sun *et al* (17) found that SENP3 was overexpressed and positively correlated with OSCC tumor differentiation.

In the present study, the role of VPA as a HDACi on the oral tongue cancer cell line, CAL27, was investigated, and its interactions with SENPs were characterized. Furthermore, the therapeutic potential of VPA in treating OSCC was examined using a xenograft model of the disease.

Materials and methods

Cell culture. Tongue cancer cell line, CAL27, was purchased from Shanghai Key Laboratory of Stomatology, Ninth People's Hospital, Shanghai Jiao Tong University School of Medicine, (Shanghai, China) and cultured in Dulbecco's Modified Eagle Medium (DMEM) supplemented with 10% fetal bovine serum (FBS; both Gibco; Thermo Fisher Scientific, Inc., Waltham, MA, USA), 100 IU/ml penicillin and 100 mg/ml streptomycin (both Invitrogen; Thermo Fisher Scientific, Inc.) at 37˚C in an atmosphere containing 5% CO_2. Cells were harvested at 80-90% confluency by trypsinization with 0.25 mg/ml trypsin/EDTA (Gibco; Thermo Fisher Scientific, Inc.), nad subsequently suspended in DMEM prior to use. Cells were incubated in DMEM for 24-48 h before treatment with VPA dissolved in DMSO (Gibco; Thermo Fisher Scientific, Inc.). Control cells were treated with DMSO only.

Cell growth assay. Viability of CAL27 cells treated with VPA was determined by standard MTT assays. Cells were seeded in 96-well plates at a density of $1x10^3$ cells per well and grown overnight in DMEM supplemented with 10% FBS, 1% glutamine and 1% penicillin-streptomycin at 37˚C and 5% CO_2. FBS-supplemented medium was removed and cells were cultured in serum-free DMEM for 2 h. VPA (99-66-1; Sigma-Aldrich; Merck Millipore, Darmstadt, Germany) was dissolved in DMSO and used at final concentrations of 0.5, 1.0, 1.5, 2.0, 2.5, and 3.0 mmol/l, respectively. Following exposure to VPA for 24, 48, 72, 96, and 120 h, respectively, supernatants were removed and 20 μl MTT solution (5 μg/ml; Sigma-Aldrich; Merck Millipore) was added to each well for an additional 4 h at 37˚C. Supernatants were subsequently discarded and 100 μl DMSO was added to each well. Absorbance was read at 540 nm using a microplate reader (Model 550; Bio-Rad Laboratories, Inc., Hercules, CA, USA). Proliferation rates were calculated by comparing the cell density of the VPA-treated cells with that of DMSO-treated cells.

Flow cytometric analysis of apoptotic cells. Apoptosis was measured by flow cytometry using a Annexin V-fluorescein isothiocyanate/PI propidium iodide (PI) apoptosis detection kit (Nanjing Keygen Biotech, Nanjing, China), according to the manufacturer's instructions. CAL27 cells ($1x10^6$) were seeded into 6-well plates and treated with VPA at final concentrations of 0.5, 1.0, 1.5, 2.0 and 3.0 mmol/l, respectively. Following treatment for 48 h, the cells were trypsinized, washed with PBS, and resuspended in 500 μl binding buffer containing Annexin V-Fluos labeling reagent and PI at $2x10^4$ cells/ml. Cells were then incubated in the dark for 15 min at room temperature and analyzed using a FACS Aria flow cytometer (BD Biosciences, Franklin, NJ, USA). For each sample, 20,000 cells were analyzed. Apoptotic rates were calculated using FlowJo 7.6.3 software (Tree Star, Inc., Ashland, OR, USA).

Flow cytometric analysis of the cell cycle. Cells ($1x10^6$) were seeded into 6-well plates and treated with VPA at final concentrations of 0.5, 1.0, 1.5, 2.0 and 3.0 mmol/l for 24 h, respectively. Cells were harvested from each well, washed in cold phosphate-buffered saline (PBS), and fixed overnight with cold 70% ethanol. Cells were then incubated with PBS buffer containing 50 μg/ml PI and 50 μg/ml RNase (both Sigma-Aldrich; Merck Millipore) for 30 min at room temperature. Cellular PI fluorescence intensity was determined using a FACS Aria flow cytometer. Data were analyzed using FlowJo software to model various cell populations. Apoptosis ratios in the VPA-treated cells were compared with those of DMSO-treated cells.

RNA isolation and reverse transcription-quantitative polymerase chain reaction (RT-qPCR) analysis. Total RNA was isolated from CAL27 cells treated with VPA at final concentrations of 0.5, 1.0, 1.5, 2.0 and 3.0 mmol/l for 12, 24, and 48 h, respectively, using TRIzol reagent (Invitrogen; Thermo Fisher Scientific, Inc.) and DNase treatment to remove genomic DNA. First strand cDNA was synthesized with 1 μg total RNA using a cDNA synthesis kit (Takara Bio, Inc., Otsu, Japan) and an RNase-free DNase kit (Qiagen, Inc., Valencia, CA, USA). Total reaction volume was 20 μl consisting of 4 μl 5X RT Buffer, 2 μl dNTP mixture, 1 μl RNase inhibitor, 1 μl Oligo $(dT)_{20}$ (Thermo Fisher Scientific, Inc.), 1 μl ReverTra Ace (Toyoba Co., Ltd., Osaka, Japan), 1 μg total RNA and RNase-free H_2O. cDNA was stored at -80˚C for the following experiments. SYBR Green (Qiagen, Inc.) was used to detect PCR products using the Bio-Rad Mini Opticon real-time PCR system in a total volume of 20 μl, consisting of 2 μl cDNA, 10 μl SYBR® Green Real-Time PCR MasterMix, 0.8 μl forward primer (10 μmol/l), 0.8 μl reverse primer (10 μmol/l), and 6.4 μl RNase-free H_2O. Reaction conditions were 95˚C for 1 min, followed by 40 cycles of 95˚C for 5 sec, 60˚C for 30 sec, and 72˚C for 45 sec, with final extension at 72˚C for 10 min. GAPDH transcripts were also analyzed for quality assurance.

Dissociation curves were calculated and gene expression levels were analyzed using the standard curve method. To normalize samples, GAPDH was used. All experiments were repeated a minimum of three times. qPCR assays were performed in 96-well optical plates, Cq values were normalized to GAPDH Cq values, and relative expression was calculated using the $2^{-\Delta\Delta Cq}$ method (18). Primer pairs were synthesized by Sangon Biotech Co., Ltd., (Shanghai, China) and are presented in Table I.

Animal studies and xenograft tumor formation assays. Four-week-old female BALB/c nu/nu mice (n=5 per group; weight, 14.5±1.87 g) were purchased from the Laboratory Animal Center of the Chinese Academy of Science

Table I. Primer sequences.

Primer	Direction	Sequence
GAPDH	Forward	5'-CTGCACCACCAACTGCTTAG-3'
	Reverse	5'-GTCTTCTGGGTGGCAGTGAT-3'
SENP1	Forward	5'-ACTGATAGTGAAGATGAATTTCCTGA-3'
	Reverse	5'-CATCCTGATTCCCATTACGAA-3'
SENP3	Forward	5'-ACTGGCTCAATGACCAGGTGATGAACATG-3'
	Reverse	5'-CCAGGTGGATGGGGATTAGCAGTAG-3'
SENP5	Forward	5'-TGCTAGATCACCTCGTCTTCA-3'
	Reverse	5'-AGTGCTTAGTGGTTTTCATGATA-3'
SUMO1	Forward	5'-GGATCCATGGCCGACGAAAAGCCCAAG-3'
	Reverse	5'-CCCGGGTCAGTAGACACCTCCCGTCTG-3'
SUMO2	Forward	5'-GACGAGAAACCCAAGGA-3'
	Reverse	5'-CTGCCGTTCACAATAGG-3'
SUMO3	Forward	5'-GGATCCATGTCCGAGGAGAAGCCCAAG-3'
	Reverse	5'-CCCGGGCTAGAAACTGTGCCCTGCCAG-3'
SAE1	Forward	5'-AGACACAGATGAATTGGCCAA-3'
	Reverse	5'-TCTGTGTCTACTTAACCGGAA-3'
SAE2	Forward	5'-GAGGTGACTGTGCGGCTGAATG-3'
	Reverse	5'-TCTTGAGCTGTGGAGGTGGAGG-3'
UBC9	Forward	5'-CAGCCATTACCATCAAACAGA-3'
	Reverse	5'-GTCGGTAATGGTAGTTTGTCT-3'

SUMO, small ubiquitin-related modifier; SENP, SUMO-specific proteases; SAE, SUMO-activating enzyme subunit; UBC, ubiquitin carrier protein.

(Shanghai, China) and maintained in a pathogen-free animal facility. Animals were placed under controlled environmental conditions in iron cages (n=5 in each cage) at 23±1˚C (60% humidity) and a 12-h dark/light cycle. Animals were subjected to acclimatization for at least one week before the experiment. They were provided with commercially available laboratory rodent diet and water was provided *ad libitum* throughout the period of the study. All experimental procedures involving animals were approved by the Animal Care and Use Committee of Zhongshan Hospital of Fudan University. CAL27 cells were collected and resuspended in DMEM, prior to subcutaneous injection into the right flank of BALB/c nude mice at a density of $5x10^6$ cells in 200 μl DMEM. When the tumors were palpable, the mice were randomly divided into control or VPA-treated groups. Control group mice received DMSO only and the VPA-treated group received 300 mg/kg VPA via intraperitoneal injection (19-21) administered daily for 28 days. Tumor volumes were regularly measured using Vernier calipers, twice per week, and calculated according to the formula: length x width x height x 0.52 (mm^3). Following treatment, the mice were immediately euthanized via cervical dislocation and tumors were excised. Tumors were washed with PBS and fixed with 4% paraformaldehyde for immunohistochemical examination and terminal deoxynucleotidyl transferase dUTP nick-end labeling (TUNEL) assay analysis.

Immunohistochemical staining. Tumor specimens from the xenograft models were cut into 5 μm slices, fixed in 10% neutral buffered formalin, and embedded in paraffin. Slides were preincubated in 5% goat serum in PBS and immunostained with anti-Ki67 (ab15580) and anti-proliferating cell nuclear antigen (PCNA; ab29) primary antibodies (both Abcam, Cambridge, UK) diluted 1:100 at 4˚C overnight. Slides were treated with hematoxylin for 30 sec for visualization under a light microscope.

TUNEL assay. Half of each xenograft tumor was fixed in 4% paraformaldehyde and embedded in paraffin. Slides were washed after deparaffinization and the sections were permeabilized with 0.1% Triton X-100 for 5 min on ice. Sections were subsequently incubated with proteinase K (Sigma-Aldrich; Merck Millipore) for 10 min at room temperature. Following this, TUNEL staining was performed using an *in situ* apoptosis detection kit (KeyGen Biotech Co., Ltd., Nanjing, China), according to the manufacturer's instructions. Sections were counterstained with hematoxylin, and TUNEL-positive cells were counted at x100 magnification in 10 randomly chosen fields using a light microscope. Results were expressed as the mean percentage of apoptotic cells.

Statistical analysis. SPSS 16.0 software (SPSS Inc., Chicago, IL, USA) was used for statistical analyses. Comparisons among the CAL27 cell cycle data sets following VPA treatment were performed using nonparametric statistical tests. Comparisons among the CAL27 cell apoptosis data were conducted using one-way analysis of variance, and post-hoc comparisons between the groups were analyzed by the least significant test. Data were expressed as the mean ± standard deviation and $P<0.05$ was considered to indicate a statistically significant difference.

Results

VPA decreases the growth of CAL27 cells in vitro. The anti-proliferative effect of VPA was examined by incubating CAL27 cells with increasing concentrations of VPA. Cell viability, as assessed by MTT assay, demonstrated appropriate concentration- and time-dependent inhibitory effects by VPA as displayed in Fig. 1. The concentrations and incubation times of VPA required for significant inhibition of cell viability ($P<0.05$) were >0.5 mmol/l and 24 h, respectively. A pronounced dose-dependent decrease in viability was observed at VPA concentrations of 0.5-3.0 mm/l at each time point from 24-120 h.

VPA induces apoptosis. The findings of the MTT assay showed that VPA reduced the viability of CAL27 cells, which suggested a relationship between cell growth and the cell cycle and/or cell apoptosis (Fig. 1). Consequently, the effects of VPA on CAL27 apoptosis were analyzed using Annexin V and PI staining assays (Fig. 2) with the same dosage range as used in the previous experiments. Cells that were positive for both Annexin V and PI positive were deemed to be in the later stages of apoptosis, while Annexin V-positive cells were in the earlier stages of apoptosis. The present findings demonstrated that CAL27 cells underwent apoptosis after 48 h of incubation with VPA in a significant and dose-dependent manner, as compared with the control ($P<0.05$).

VPA-induces cell cycle arrest. To investigate the effect of VPA on the cell cycle of CAL27 cells, flow cytometry experiments were performed. The results indicated that cells treated with 0.5, 1.0, 1.5, 2.0 and 3.0 mmol/l VPA, respectively, were in the S phase for less time than the control cells. G_1 cell populations increased significantly at these concentrations of VPA, compared with the control cells ($P<0.05$; Fig. 3; Table II).

VPA increases the mRNA expression levels of various SUMOylation genes. To determine the effect of VPA on CAL27 inhibition, RT-qPCR was used to demonstrate that SUMO1 and SUMO2 mRNA expression significantly increased with the increasing VPA dosage ($P<0.01$). A significant increase in SENP3 was also detected after 48-h treatment with 1.0, 1.5, 2.0 and 3.0 mmol/l VPA ($P<0.01$). In contrast, expression of SENP1 initially decreased, declining to a minimum at 24 h, and subsequently exhibited a significant increase at 24 h with 1.0 and 1.5 mmol/l VPA ($P<0.01$). mRNA expression levels of SAE1, SAE2, SUMO3, SENP5 and UBC9 were also measured; however, but no significant dose- and/or time-dependent effects were observed (Fig. 4).

VPA reduces the speed of tumor growth in vivo. To further evaluate the therapeutic potential of VPA *in vivo*, a xenograft model was established in nude mice via subcutaneous injection of CAL27 cells. The volumes of established tumors were examined every four days, and the time course of changes in xenografted tumor volumes are shown in Fig. 5. Following treatment with VPA, tumors generated from CAL27 cells grew more slowly than control tumors treated with the vehicle only.

VPA decreases proliferation potential and increases apoptosis in xenograft tumors in vivo. Ki67 and PCNA

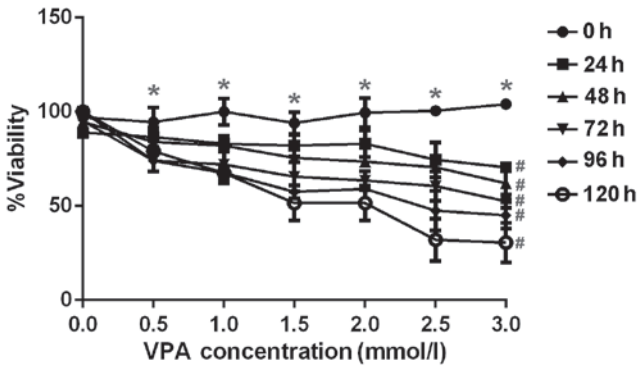

Figure 1. Inhibitory effect of various doses of VPA on CAL27 cell proliferation. CAL27 cells were treated with 0.5, 1.0, 1.5, 2.0, 2.5 and 3.0 mm/l VPA for 24, 48, 72, 96 and 120 h, respectively, *in vitro*. Cell viability was determined using MTT assay and analyzed as the percentage of the absorbance value compared with control. *P<0.05 vs. 0.0 mmol/l; #P<0.05 vs. 0 h. Error bars represent the standard error of the mean. VPA, valproic acid.

are considered to be pivotal markers of tumor proliferation (22,23). Xenograft tumors were fixed with formalin and embedded in paraffin, followed by immunohistochemistry to visualize the expression levels of both markers. Representative images of the immunohistochemical findings for Ki67 and PCNA are shown in Fig. 6, indicating the decreased expression of both proteins in the tumors of VPA-treated mice. The effect of VPA on apoptosis in xenograft tumors originating from CAL27 cells was also characterized by a TUNEL assay. Representative results are presented in Fig. 7, demonstrating increased DNA fragmentation in the sections from VPA-treated mice as a result of activated apoptotic signaling cascades.

Discussion

The function of VPA in various malignant tumors has been widely studied in recent years. As such, it has been demonstrated that treatment with VPA induces a significant reduction in tumor proliferation through the induction of S phase arrest (24), and this anticancer effect may have been acquired through the alteration of cell cycle proteins, including cyclins D1 and D3 and cyclin-dependent kinase 4 (25). Previous studies have also indicated that VPA markedly increased the enrichment of reactive oxygen species in leukemia cells, which led to the upregulation of growth inhibitory pathway (26,27). Ki67, as a functional component of proliferating cells during mitosis, was reduced by VPA in murine neural stem cells, resulting in growth inhibitory effects (28). In addition, VPA also induced a significant reduction in tumor proliferation through the induction of apoptosis (29). Previous investigation in leukemia cells demonstrated that inhibition of HDAC activity by VPA led to the induction of apoptosis via the disturbance of normal epigenetic processes (29). Furthermore, studies have confirmed that VPA treatment resulted in the induction of differentiation in murine neural stem cells and some malignant cells via HDAC inhibition (30-32). Thus, the anticancer effects of VPA have been well-documented.

Oral squamous cell carcinoma is the most frequently occurring malignant oral tumor in the oral cancer group (2); however,

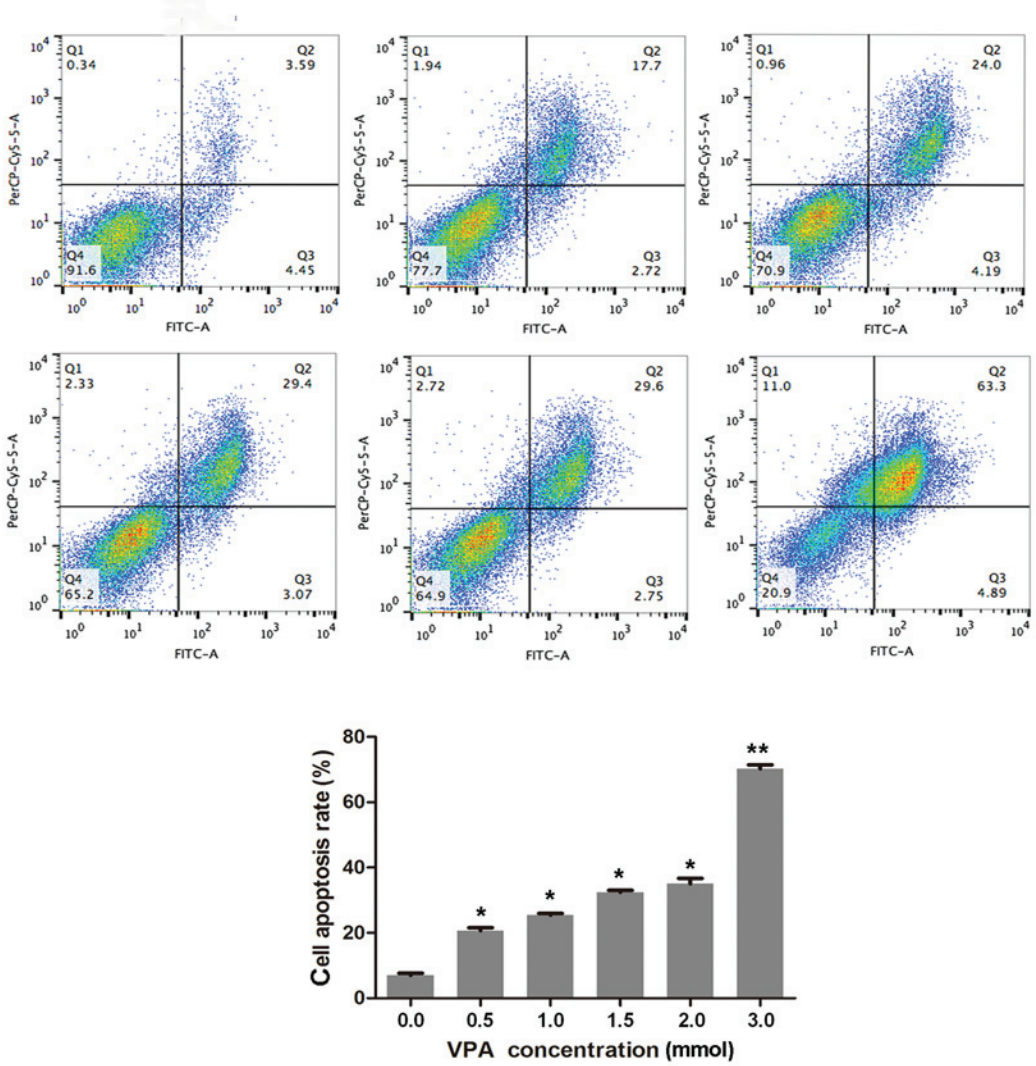

Figure 2. Flow cytometric analysis of various doses of VPA on CAL27 cells apoptosis. CAL27 cells were incubated with 0.5, 1.0, 1.5, 2.0, 2.5 and 3.0 mm/l VPA for 48 h, respectively, and apoptotic cells were stained with propidium iodide and measured by flow cytometry. *P<0.05; **P<0.01. VPA, valproic acid.

to the best of our knowledge, the effectiveness of VPA on OSCC has not been widely investigated. In the present study, the effects of VPA on OSCC were examined *in vivo* and *in vitro*. Treatment with VPA inhibited the growth of CAL27 cells and xenografted OSCC. This effect may be attributed to VPA-induced increases in G_1 phase arrest rates as well as elevated rates of apoptosis in carcinoma cells. The inhibitory effects of VPA on OSCC were manifested by its effects on the viability, differentiation, and apoptosis of cancer cells, which is consistent with previous research (33).

Post-translational modification has emerged as an important method of regulating the extent of cellular signaling by pathway components (34). For example, the specific acetylation activity pattern of SUMO was shown to alter protein phosphorylation patterns, thus affecting the activity of certain regulatory proteins (35). It has been hypothesized that SENPs modulate the cell cycle and tumorigenesis, utilizing divergent mechanisms (36-38). In the present study, SUMO modification of mRNA expression levels in CAL27 cells differed according to the VPA concentration. The mRNA expression level sof SUMO ligases, SAE1 and SAE2, exhibited no significant alterations. Moreover, the mRNA

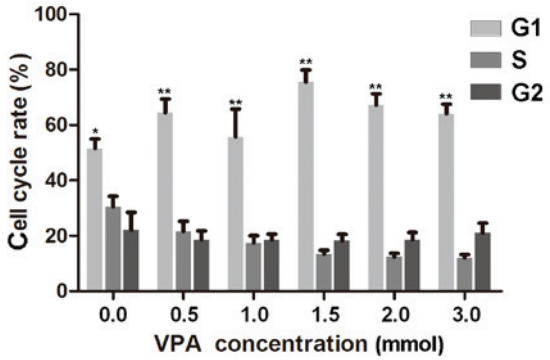

Figure 3. Statistical analysis of the effect of various doses of VPA on the cell cycle of CAL27 cells over 24 h compared with the control. *P<0.05; **P<0.01. VPA, valproic acid.

expression levels of SUMO1 and SUMO2 in CAL27 cells exposed to different concentrations of VPA did not initially change after 24 h exposure, but rose rapidly after 48 h with 1.0 and 1.5 mmol/l VPA. Treatment with VPA at 1.0, 1.5, and 3.0 mmol/l produced fold changes of 1.8, 2.2, 2.1 and

Table II. Alterations in the cell cycle progression of CAL27 cells after treatment with VPA for 24 h.

Phase	Control group	0.5 mm/l VPA	1 mm/l VPA	1.5 mm/l VPA	2 mm/l VPA	3 mm/l VPA	P-value
G0/G1	51.53±5.99	64.43±8.89	62.24±6.76	75.63±7.38	67.66±7.07	64.31±6.26	<0.05
S	30.66±6.56	21.5±6.92	17.42±4.70	13.3±2.57	12.41±2.34	12.25±2.56	<0.05
G2/M	22.43±11.00	18.85±5.76	18.71±3.27	21.65±7,14	18.86±4.46	21.18±5.99	>0.05

VPA, valproic acid.

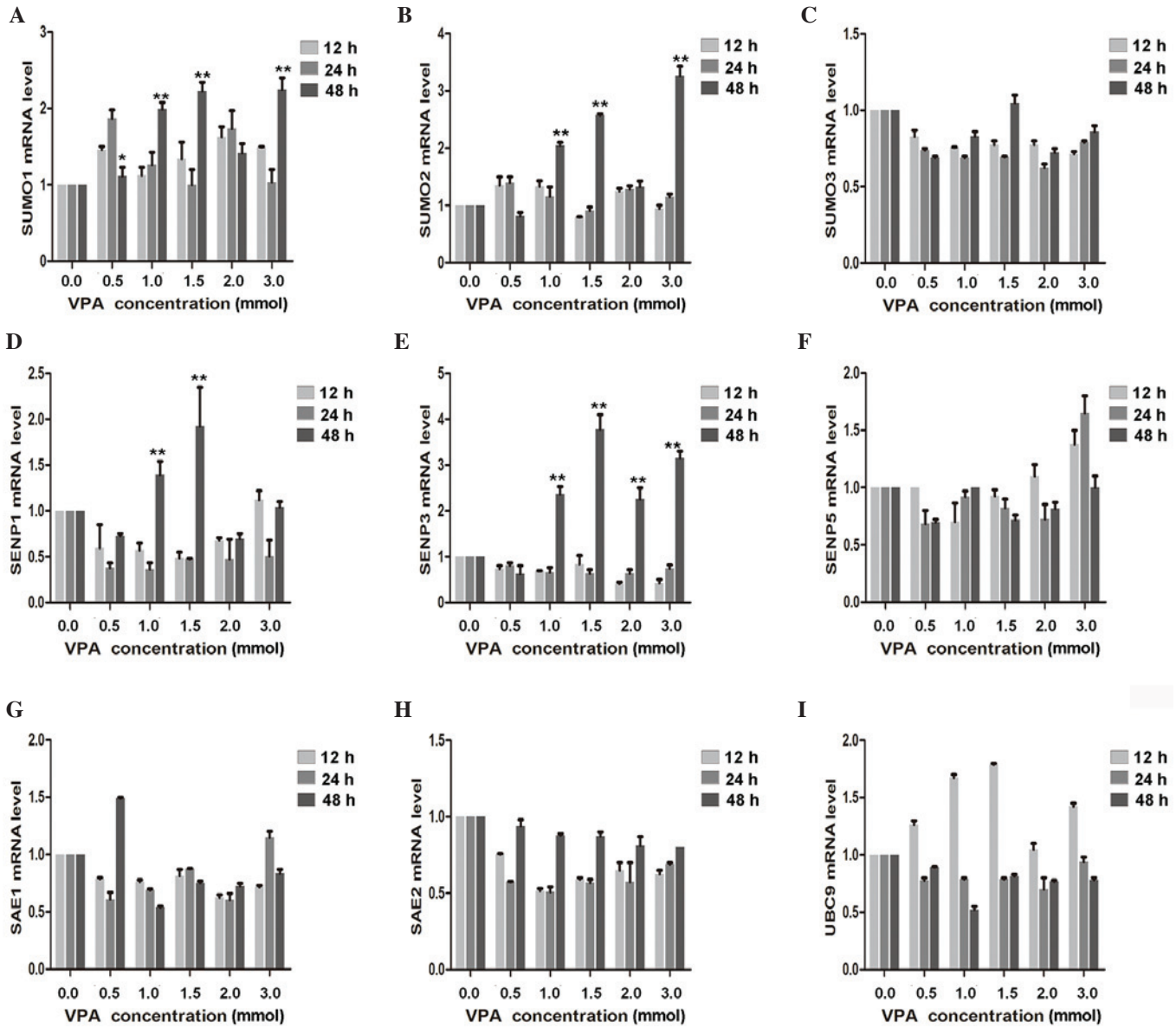

Figure 4. Effect of VPA on related genes. Reverse transcription-quantitative polymerase chain reaction results of known tumor suppressor genes, including (A) SUMO1, (B) SUMO2, (C) SUMO3, (D) SENP1, (E) SENP3, (F) SENP5, (G) SAE1, (H) SAE2 and (I) UBC9 in VPA-incubated CAL27 cells compared with the control. *P<0.05; **P<0.01. VPA, valproic acid.

2.1, 2.6, 3.0-fold in SUMO1 and SUMO2 mRNA expression levels, respectively,. At 1.0, 1.5 and 3.0 mmol/l VPA, the changes in the mRNA expression levels of SUMO1 and SUMO2 were statistically significant. Regarding SENP mRNA expression, the findings of the present study showed that SENP1 mRNA expression levels transiently declined 12 h after VPA exposure regardless of the concentration used. In contrast, mRNA expression levels of SENP3 were significantly increased following 48 h exposure to 1.0, 1.5, 2.0 and 3.0 mmol/l VPA. SENP5 mRNA expression levels were not demonstrated to be statistically correlated with VPA concentration or exposure time.

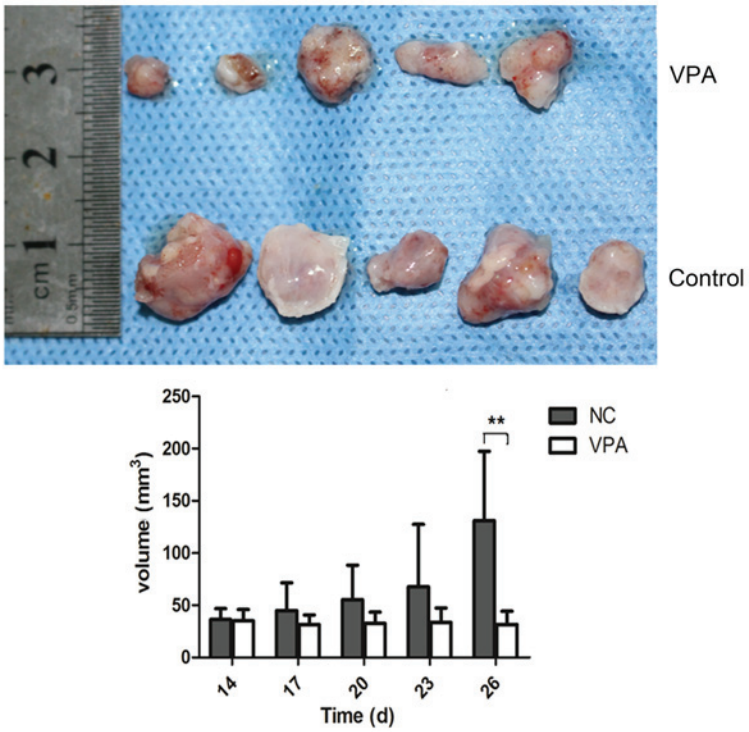

Figure 5. Inhibitive effect of VPA on the growth of tumor xenografts. Once the tumors were palpable, the mice were randomly divided into control or VPA-treated groups. Drug injections were administered daily for 28 days. Tumors size was measured using vernier caliper and the volumes were calculated by formula: length x width x height x 0.52 (mm^3). $^{**}P<0.01$. VPA, valproic acid.

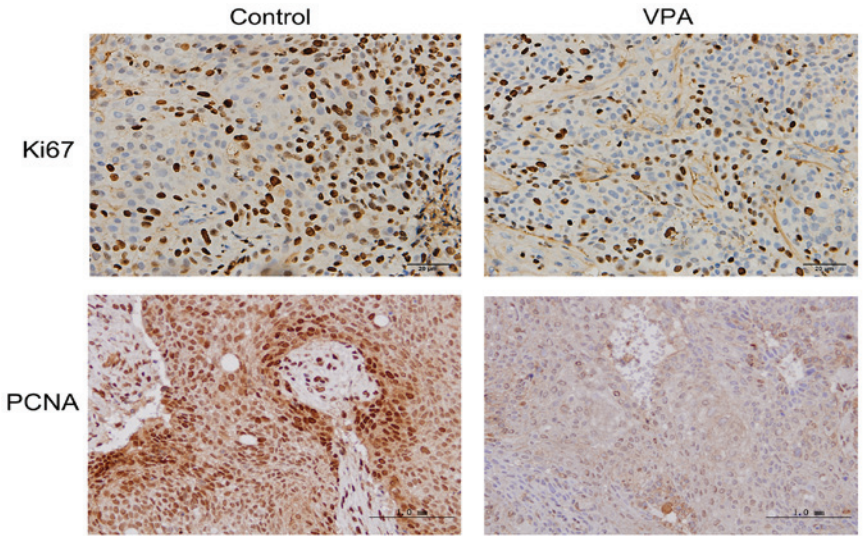

Figure 6. Immunohistochemistry for Ki67 and PCNA in xenograft tumors *in vivo*. Ki67 staining was strong in the tumor cells and reduced in tumor tissue of mice treated with VPA. Similar expression patterns were observed for the staining of PCNA. Magnification, x100. PCNA, proliferating cell nuclear antigen.

The alterations in SUMO and SENP expression levels observed in the present study suggest that SUMO modifications are not involved in the early differentiation of OSCC induced by VPA. One possible reason is that SUMO modification and conversion occur on different proteins. While some proteins may be selectively SUMOylated, SUMO modifications do not increase overall and SENP1 and SENP3 may have important roles in regulating the timing of SUMO modifications. However, position changes of SUMO proteins and SUMO-related proteins SENP1, SENP3, SENP5 were not examined in the present study. Therefore, the cellular location and volume changes of SUMO-related proteins should be examined in future studies in order to fully elucidate the specific mechanisms.

In conclusion, VPA, which is a HDACi, was demonstrated to be associated with cell cycle inhibition and apoptosis induction in OSCC. Targeted therapy with VPA may decrease cell viability and induce significant antitumor effects by promoting the differentiation of OSCC. These findings indicate that VPA may be useful for the clinical treatment of OSCC, and

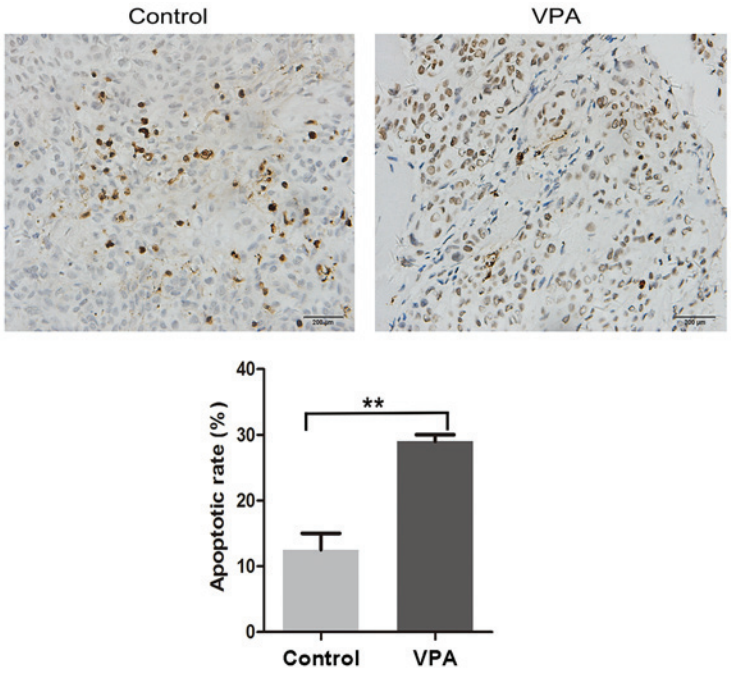

Figure 7. Cell proliferation of tumor xenografts was analyzed by TUNEL assay. Representative images present TUNEL-stained tumors from control and VPA-treated mice, respectively. Magnification, x100. Results indicated that apoptosis was significantly increased in the VPA-treated tumors, as compared with the DMSO control-treated tumors. **P<0.01. TUNEL, terminal deoxynucleotidyl transferase dUTP nick-end labeling.

that alterations in SUMO-related pathway may mediate the anti-cancer effect of VPA.

References

1. Carvalho AL, Nishimoto IN, Califano JA and Kowalski LP: Trends in incidence and prognosis for head and neck cancer in the United States: A site-specific analysis of the SEER database. Int J Cancer 114: 806-816, 2005.
2. Chu W, Song X, Yang X, Ma L, Zhu J, He M, Wang Z and Wu Y: Neuropilin-1 promotes epithelial-to-mesenchymal transition by stimulating nuclear factor-kappa B and is associated with poor prognosis in human oral squamous cell carcinoma. PLoS One 9: e101931, 2014.
3. Lafon-Hughes L, Di Tomaso MV, Méndez-Acuña L and Martinez-López W: Chromatin-remodelling mechanisms in cancer. Mutat Res 658: 191-214, 2008.
4. Backs J and Olson EN: Control of cardiac growth by histone acetylation/deacetylation. Circ Res 98: 15-24, 2006.
5. Ito K, Ito M, Elliott WM, Cosio B, Caramori G, Kon OM, Barczyk A, Hayashi S, Adcock IM, Hogg JC and Barnes PJ: Decreased histone deacetylase activity in chronic obstructive pulmonary disease. N Engl J Med 352: 1967-1976, 2005.
6. Brandl A, Wagner T, Uhlig KM, Knauer SK, Stauber RH, Melchior F, Schneider G, Heinzel T and Krämer OH: Dynamically regulated sumoylation of HDAC2 controls p53 deacetylation and restricts apoptosis following genotoxic stress. J Mol Cell Biol 4: 284-293, 2012.
7. Xu WS, Parmigiani RB and Marks PA: Histone deacetylase inhibitors: Molecular mechanisms of action. Oncogene 26: 5541-5552, 2007.
8. Li Y, Liu T, Ivan C, Huang J, Shen DY, Kavanagh JJ, Bast RC Jr, Fu S, Hu W and Sood AK: Enhanced cytotoxic effects of combined valproic acid and the aurora kinase inhibitor VE465 on gynecologic cancer cells. Front Oncol 3: 58, 2013.
9. Wedel S, Hudak L, Seibel JM, Makarević J, Juengel E, Tsaur I, Wiesner C, Haferkamp A and Blaheta RA: Impact of combined HDAC and mTOR inhibition on adhesion, migration and invasion of prostate cancer cells. Clin Exp Metastasis 28: 479-491, 2011.
10. Dong LH, Cheng S, Zheng Z, Wang L, Shen Y, Shen ZX, Chen SJ and Zhao WL: Histone deacetylase inhibitor potentiated the ability of MTOR inhibitor to induce autophagic cell death in Burkitt leukemia/lymphoma. J Hematol Oncol 6: 53, 2013.
11. Mazurkiewicz-Beldzińska M, Szmuda M and Matheisel A: Long-term efficacy of valproate versus lamotrigine in treatment of idiopathic generalized epilepsies in children and adolescents. Seizure 19: 195-197, 2010.
12. Ullmann R, Chien CD, Avantaggiati ML and Muller S: An acetylation switch regulates SUMO-dependent protein interaction networks. Mol Cell 46: 759-770, 2012.
13. Wilkinson KA and Henley JM: Mechanisms, regulation and consequences of protein SUMOylation. Biochem J 428: 133-145, 2010.
14. Drag M and Salvesen GS: DeSUMOylating enzymes-SENPs. IUBMB Life 60: 734-742, 2008.
15. Katayama A, Ogino T, Bandoh N, Takahara M, Kishibe K, Nonaka S and Harabuchi Y: Overexpression of small ubiquitin-related modifier-1 and sumoylated Mdm2 in oral squamous cell carcinoma: Possible involvement in tumor proliferation and prognosis. Int J Oncol 31: 517-524, 2007.
16. Ding X, Sun J, Wang L, Li G, Shen Y, Zhou X and Chen W: Overexpression of SENP5 in oral squamous cell carcinoma and its association with differentiation. Oncol Rep 20: 1041-1045, 2008.
17. Sun Z, Hu S, Luo Q, Ye D, Hu D and Chen F: Overexpression of SENP3 in oral squamous cell carcinoma and its association with differentiation. Oncol Rep 29: 1701-1706, 2013.
18. Livak KJ and Schmittgen TD: Analysis of relative gene expression data using real-time quantitative PCR and the 2-ΔΔCt method. Methods 25: 402-408, 2001.
19. Xing B, Liang XP, Liu P, Zhao Y, Chu Z and Dang YH: Valproate inhibits methamphetamine induced hyperactivity via glycogen synthase kinase 3β signaling in the nucleus accumbens core. PLoS One 10: e128068, 2015.
20. Xing B, Zhao Y, Zhang H, Dang Y, Chen T, Huang J and Luo Q: Microinjection of valproic acid into the ventrolateral orbital cortex exerts an antidepressant-like effect in the rat forced swim test. Brain Res Bull 85: 153-157, 2011.
21. Zhao Y, Xing B, Dang YH, Qu CL, Zhu F and Yan CX: Microinjection of valproic acid into the ventrolateral orbital cortex enhances stress-related memory formation. PLoS One 8: e52698, 2013.
22. Garcia H, Fleyshman D and Kolesnikova K, Safina A, Commane M, Paszkiewicz G, Omelian A, Morrison C and Gurova K: Expression of FACT in mammalian tissues suggests its role in maintaining of undifferentiated state of cells. Oncotarget 2: 783-796, 2011.
23. Tripi TR, Bonaccorso A, Rapisarda E and Bartoloni G: Proliferative activity in periapical lesions. Aust Endod J 29: 31-33, 2003.

24. Praefcke GJ, Hofmann K and Dohmen RJ: SUMO playing tag with ubiquitin. Trends Biochem Sci 37: 23-31, 2012.
25. Juengel E, Makarević J, Tsaur I, Bartsch G, Nelson K, Haferkamp A and Blaheta RA: Resistance after chronic application of the HDAC-inhibitor valproic acid is associated with elevated Akt activation in renal cell carcinoma in vivo. PLoS One 8: e53100, 2013.
26. Miller CP, Ban K, Dujka ME, McConkey DJ, Munsell M, Palladino M and Chandra J: NPI-0052, a novel proteasome inhibitor, induces caspase-8 and ROS-dependent apoptosis alone and in combination with HDAC inhibitors in leukemia cells. Blood 110: 267-277, 2007.
27. Boku S, Nakagawa S and Masuda T, Nishikawa H, Kato A, Takamura N, Omiya Y, Kitaichi Y, Inoue T, Kusumi I: Valproate recovers the inhibitory effect of dexamethasone on the proliferation of the adult dentate gyrus-derived neural precursor cells via GSK-3beta and beta-catenin pathway. Eur J Pharmacol 723: 425-430, 2014.
28. Brunn J, Wiroth V, Kowalski M, Runge U and Sabolek M: Valproic acid in normal therapeutic concentration has no neuroprotective or differentiation influencing effects on long term expanded murine neural stem cells. Epilepsy Res 108: 623-633, 2014.
29. Valdés-Mora F, Song JZ, Statham AL, Strbenac D, Robinson MD, Nair SS, Patterson KI, Tremethick DJ, Stirzaker C and Clark SJ: Acetylation of H2A.Z is a key epigenetic modification associated with gene deregulation and epigenetic remodeling in cancer. Genome Res 22: 307-321, 2012.
30. Liu S, Klisovic RB, Vukosavljevic T, Yu J, Paschka P, Huynh L, Pang J, Neviani P, Liu Z, Blum W, *et al*: Targeting AML1/ETO-histone deacetylase repressor complex: A novel mechanism for valproic acid-mediated gene expression and cellular differentiation in AML1/ETO-positive acute myeloid leukemia cells. J Pharmacol Exp Ther 321: 953-960, 2007.
31. Leiva M, Moretti S, Soilihi H, Pallavicini I, Peres L, Mercurio C, Dal Zuffo R, Minucci S and de Thé H: Valproic acid induces differentiation and transient tumor regression, but spares leukemia-initiating activity in mouse models of APL. Leukemia 26: 1630-1637, 2012.
32. Driever PH, Wagner S, Hofstädter F and Wolff JE: Valproic acid induces differentiation of a supratentorial primitive neuroectodermal tumor. Pediatr Hematol Oncol 21: 743-751, 2004.
33. Gan CP, Hamid S, Hor SY, Zain RB, Ismail SM, Mustafa W, Mahadzir W, Teo SH, Saunders N and Cheong SC: Valproic acid: Growth inhibition of head and neck cancer by induction of terminal differentiation and senescence. Head Neck 34: 344-353, 2012.
34. Suzuki T, Yokozaki H, Kuniyasu H, Hayashi K, Naka K, Ono S, Ishikawa T, Tahara E and Yasui W: Effect of trichostatin A on cell growth and expression of cell cycle- and apoptosis-related molecules in human gastric and oral carcinoma cell lines. Int J Cancer 88: 992-997, 2000.
35. Cappadocia L, Mascle XH, Bourdeau V, Tremblay-Belzile S, Chaker-Margot M, Lussier-Price M, Wada J, Sakaguchi K, Aubry M, Ferbeyre G and Omichinski JG: Structural and functional characterization of the phosphorylation-dependent interaction between PML and SUMO1. Structure 23: 126-138, 2015.
36. Sharma P, Yamada S, Lualdi M, Dasso M and Kuehn MR: Senp1 is essential for desumoylating Sumo1-modified proteins but dispensable for Sumo2 and Sumo3 deconjugation in the mouse embryo. Cell Rep 3: 1640-1650, 2013.
37. Madu IG, Namanja AT, Su Y, Wong S, Li YJ and Chen Y: Identification and characterization of a new chemotype of noncovalent SENP inhibitors. ACS Chem Biol 8: 1435-1441, 2013.
38. Wen D, Xu Z, Xia L, Liu X, Tu Y, Lei H, Wang W, Wang T, Song L, Ma C, *et al*: Important role of SUMOylation of Spliceosome factors in prostate cancer cells. J Proteome Res 13: 3571-3582, 2014.